HLA-B27 alters BMP/TGFβ signalling in Drosophila, revealing putative pathogenic mechanism for spondyloarthritis

Benjamin Grandon, Aurore Rincheval-Arnold, Nadège Jah, Jean-Marc Corsi, Luiza M Araujo, Simon Glatigny, Erwann Prevost, Delphine Roche, Gilles Chiocchia, Isabelle Guénal, et al.

HLA-B27 alters BMP/TGFβ signaling in *Drosophila*, revealing putative pathogenic mechanism for spondyloarthritis

Authors names and affiliations

Benjamin Grandon [1,2,3], Aurore Rincheval-Arnold [1], Nadège Jah [2,3], Jean-Marc Corsi [1], Luiza M. Araujo [2,3], Simon Glatigny [2,3], Erwann Prévost [1,2], Delphine Roche [1], Gilles Chiocchia [2,3], Isabelle Guénal [1]*, Sébastien Gaumer [1]*, Maxime Breban [2,3,4]*

[1] Laboratoire de Génétique et Biologie Cellulaire, UVSQ, Université Paris-Saclay, EPHE, PSL Research University, Montigny-le-Bretonneux, France, France;

[2] UMR1173 Inserm, UVSQ, Université Paris-Saclay, Montigny-le-Bretonneux, France;

[3] INFLAMEX, Laboratoire d'Excellence, Université Paris Diderot, Sorbonne Paris Cité, Paris, France;

[4] Ambroise-Paré Hospital, Rheumatology department, AP-HP, Boulogne-Billancourt, France.

*These authors contributed equally to this work.

Corresponding author:

Maxime Breban, M.D, Ph.D.

UMR 1173 Inserm/UVSQ, 2 ave de la Source de la Bièvre, Montigny-le-Bretonneux, France and Service de Rhumatologie, Hôpital Ambroise Paré, AP-HP, 9 ave Charles de Gaulle, Boulogne-Billancourt, France. Phone #:+33 149095672.

E-mail: maxime.breban@aphp.fr

Word count: 4,194

Abstract

Objectives: The human leucocyte antigen (HLA)-B27 confers increased risk of spondyloarthritis (SpA) by unknown mechanism. The objective of this work was to uncover HLA-B27 non-canonical properties that could explain its pathogenicity, using a new *Drosophila* model.

Methods: We produced transgenic *Drosophila* expressing the SpA-associated HLA-B*27:04 or HLA-B*27:05 subtypes, or the non-associated HLA-B*07:02 allele, alone or in combination with human β2-microglobulin (hβ2m), under tissue-specific drivers. Consequences of transgenes expression in *Drosophila* were examined and affected pathways were investigated by genetic interaction experiments. Predictions of the model were further tested in immune cells from SpA patients.

Results: Loss of crossveins in the wings and a reduced eye phenotype were observed after expression of HLA-B27:04 or HLA-B*27:05 in *Drosophila* but not in fruit flies expressing the non-associated HLA-B*07:02 allele. These HLA-B27-induced phenotypes required the presence of hβ2m that allowed expression of well-folded HLA-B conformers at the cell surface. Loss of crossveins resulted from a dominant negative effect of HLA-B27 on the type I bone morphogenetic protein (BMP) receptor Saxophone (Sax) with which it interacted, resulting in elevated Mother against dpp (Mad, a *Drosophila* receptor-mediated Smad) phosphorylation. Likewise, in immune cells from SpA patients, HLA-B27 specifically interacted with activin receptor-like kinase-2 (ALK2), the mammalian Sax ortholog, at the cell surface and elevated Smad phosphorylation was observed in response to Activin A and transforming growth factor β (TGFβ).

Conclusions: Antagonistic interaction of HLA-B27 with ALK2, which exerts inhibitory functions on the TGFβ/BMP signaling pathway at the cross-road between inflammation and ossification, could adequately explain SpA development.

Keywords: Ankylosing Spondylitis; Spondyloarthritis; HLA-B27; TGFβ; BMP; ALK2

Introduction

The class I major histocompatibility complex (MHC-I) allele encoding HLA-B27 is the main genetic factor predisposing to ankylosing spondylitis (AS) and the related spondyloarthritis (SpA). This is a group of frequent disabling diseases primarily characterized by chronic inflammation of the axial skeleton, leading to bony ankylosis of the sacroiliac and vertebral joints.[1] Strong association between AS and HLA-B27 was first described 46 years ago[2] but still remains largely unexplained.

Upon synthesis, MHC-I heavy chain enters the endoplasmic reticulum (ER) where it associates non-covalently with both the invariant hβ2m chain and a 8 to 10-mer peptide before being exported to the cell surface *via* the Golgi apparatus.[3] The canonical function of HLA-B molecules is to present antigenic peptides derived from cytosolic proteins to CD8+ T cells, leading to a cytotoxic response.[4] Accordingly, one of the oldest theories that was proposed to explain HLA-B27 pathogenicity, also designated as the "arthritogenic peptide" hypothesis, speculates on the capacity of this molecule to specifically present as yet undetermined antigenic peptide(s) derived from the joint, thereby triggering a harmful CD8+ T cell-mediated response.[5] However, convincing evidence supporting the implication of such mechanism is still lacking. Other theories have emerged more recently, based on non-canonical biological features of HLA-B27. These include the formation of homodimers of HLA-B27 heavy chains at the cell surface, interacting with killer immunoglobulin-like receptors expressed on CD4+ T cells and natural killer cells.[4] Alternatively, failure of HLA-B27 to fold properly during its assembly may lead to an ER stress response, thereby fostering chronic inflammation.[6] However, none of these hypotheses has been fully proven yet.

Drosophila melanogaster is an invaluable system to understand complex molecular mechanisms.[7] Indeed, many cellular signaling pathways and functions are conserved between mammals and *Drosophila*. Here, we speculated that this simple experimental live system could be suitable to unravel aberrant functional consequences of HLA-B27/hβ2m expression, that could contribute to its pathogenicity.

Methods

Drosophila lines. *Drosophila* were cultured using standard corn-agar medium. Crosses were performed at 25°C. Various GAL4 drivers used to induce transgenes expression and origin of the stocks are described in **Supplementary Table 1**.

Transgenic lines constructs. Flies carrying the cDNA of either *HLA-B*27:04*, *HLA-B*27:05*, *HLA-B*07:02*, or *hβ2m*, under control of UAS regulatory sequences that can be bound by the yeast GAL4 transcription factor to direct tissue-specific expression were generated by *P*-element transgenesis.[8] Human cDNAs containing the full-length coding region have been previously described.[9] They were ligated in the pUASg-attB vector (Gateway® Technology). The resulting plasmids were purified with Qiagen tips and sent for injection into *w^1118* embryos (BestGene Inc, California, USA). *UAS-HLA-B*07:02*, *UAS-HLA-B*27:05*, and *UAS-HLA-B*27:04* transgenes were all inserted as single copy in the same predefined site (68A4 of chromosome 3) allowing to control for the non-specific consequence of the insertion, when comparing different HLA-B transgenes. *UAS-hβ2m* was inserted in 89E11 of chromosome 3. At least two independent transgenic lines were studied for each single or recombined transgene, leading to identical phenotype. Effective expression of the transgenes was observed at the transcription and protein levels by real-time quantitative PCR (RT-q-PCR) and Western-blot, respectively **(Supplementary Fig. 1a-c)**.

Genetic interaction tests. The effect of *HLA-B*27:05/hβ2m* expression driven by *nub-Gal4* was assayed in different genetic backgrounds to test for the interaction of *HLA-B*27:05 with* different candidate genes. *nub-Gal4> UAS-HLA-B*27:05, UAS-hβ2m Drosophila* females were crossed with males bearing a loss-of-function or overexpressing mutant alleles of these genes. Each test was done thrice in independent experiments. For wing phenotype analysis, all the progeny was analyzed for each cross, including 40 to 100 flies. The phenotype of each cross was fully penetrant. About ten adult wings were dissected from random adult flies in PBS and mounted with 50% glycerol. Images were obtained with a LEICA MZFLIII microscope and an Olympus DP20 Digital Color Camera

(Olympus, Hamburg, Germany). Scale information was recorded in the image. For wing imaginal discs, the number of imaginal discs analyzed was indicated on the corresponding graph.

RNA extraction and RT-qPCR. Forty wing imaginal discs were dissected in the RNA XS NucleoSpin kit's lysis buffer (Macherey-Nagel, Düren, Germany) on ice for each genotype to extract total RNAs. RNA concentration was determined by NanoDrop 1000 (ThermoScientific, Wilmington, USA). Reverse transcription was performed using 500 *ng* of total RNA following the protocol of M-MLV Reverse Transcriptase (ThermoScientific, Wilmington, USA). RT-qPCR was performed using the CFX96 Touch[TM] Real-Time PCR Detection System. Reaction mix preparation is composed of iTaq[TM] Universal SYBR®Green Supermix (BIORAD, Hercules, USA)) and 11 ng of cDNA as described in Biorad reaction mix preparation protocol. Three independent RT-qPCR experiments were performed and data were normalized against *uba2* mRNA levels. Forward and reverse primer sequences (Invitrogen, Life Technologies) used for RT-qPCR are shown in **Supplementary Table 2**.

Immunostaining and microscopy. Wing discs of third-instar larvae were dissected and immunostained as previously described.[10] The following primary antibodies (Abs) were used: rabbit anti-Death caspase-1 (Dcp-1 Asp216, Cell Signaling, Danvers, MA, USA, 1:50);[11] rabbit anti-p-Smad1/5 to detect phosphorylated Mother against dpp (p-Mad, S463/465, Cell Signaling, Danvers, MA, USA, 1:100);[12] rabbit anti-GFP (A-11122, ThermoFisher Scientific, MA, USA, 1:500); rabbit anti-HA tag (Y-11, Santa Cruz, Dallas Texas, USA, 1:500); HC-10, a mouse IgG2a monoclonal Ab (mAb) recognizing unfolded HLA-B heavy chains;[13] ME1, a mouse IgG1 mAb that is specific for properly folded HLA-B27, HLA-B7 and HLA-B22 proteins;[14] w6/32, a mouse IgG2a mAb uniformly recognizing a monomorphic determinant of all folded HLA-A, -B and -C proteins (ab22432, Abcam)[15] and BBM1 a mouse anti-hβ2m IgG2b mAb.[16] Secondary Abs conjugated to Alexa Fluor 488, 568 or 647 were purchased from Molecular Probes (Eugen, OR, USA 1:400). Discs were mounted in Citifluor (Biovalley, Marne-La-Vallée, France). Images were captured using a Leica SPE confocal laser-scanning microscope (Leica, Wetzlar, Germany). Images were stacked and mean intensity was quantified with the ImageJ software.

Eye size measurement. Two- to 3-day-old adult flies were immobilized by freezing at -80°C and mounted on a Petri dish before being imaged at 3.2X magnification using a LEICA MZFLIII microscope and an Olympus DP20 Digital Color Camera (Olympus, Hamburg, Germany). Eye size was measured with the ImageJ pixel area function.

Imaginal disc cell preparation for flow cytometry. Thirty wing discs were dissected in phosphate-buffered saline (PBS) and transferred to siliconized tubes for trypsinization during 1.5 hours at 25°C (90% Trypsin in PBS, Thermofisher). Transgene expressing cells were also expressing GFP. Dissociated cells were left 2.5 hours in Schneider medium at 25°C and incubated with the primary Ab diluted in PBS + bovine serum albumin 0.1% for 30 min at room temperature (RT). Cells were then rinsed and incubated with the secondary Ab and propidium iodide (PI) for 30 min at RT. PI- and GFP+ cells were characterized with a FACSCanto II system (FORTESSA, BD Biosciences) and analyzed thanks to the Flowjo software (Tree Star).

Proximity ligation assay (PLA). PLA was performed using the Duolink In Situ Red Starter Kit Mouse/Rabbit (Sigma-Aldrich), following the manufacturer's protocol. For *Drosophila* experiments, twenty wing imaginal discs for each genotype were dissected in PBS, fixed in 3.7% formaldehyde for 20 min at RT and permeabilized in PBS + Tween 0.3%. Primary anti-HA (rabbit, Y11 Santa Cruz), and w6/32 Abs were used overnight at 4°C. For B-LCL experiments, anti-ALK2 (Sigma-Aldrich, 1:100), anti-CD45 (mouse, 2B11 + PD7/26, Dako, California, USA, 1:100), ME1 and w6/32 Abs were used. Ten random 40x images per condition were acquired using the DAPI (blue nuclei) and Cy5 (red PLA signals) filters. Z-stack confocal images were collected and maximum intensity projections were generated by ImageJ. Automatic counting of the PLA dots using the "Find Maxima" function in ImageJ software were performed.

Human cells: Lymphoblastoïd B cell lines (B-LCLs) *10151* (HLA-A*02, *31; B*27:05, *15; C*02, *03), *6370* (HLA-A*02, *68; B*27:05, *44; C*02, *07), and *13617* (HLA-A*02, *03; B*27:05, *18; C*02, *07) were established from AS patients and have been previous described.[17,18] B-LCLs *9435* (HLA-A*02, *03; B*07, *44; C*05, *07), *9953* (HLA-A*03, *30; B*07, *49; C*06, *07) and *6908*

(HLA-A*02, *11; B*22, *44; C*03, *05) were established from Epstein-Barr virus-transformed lymphocytes from healthy controls according to standard protocol and grown at 37°C in RPMI 1640 medium supplemented with 10% heat inactivated fetal bovine serum, 100 U/mL penicillin and 100 µg/mL streptomycin. Peripheral blood mononuclear cells (PBMC) were isolated from HLA-B27+ SpA patients and HLA-B27 negative healthy controls, having signed informed consent, by Ficoll (GE Healthcare) density gradient centrifugation. CD14+ cells were first removed from PBMC by positive magnetic selection, using anti-CD14 microbeads and AutoMacs Pro Separator (Miltenyi Biotec). The characteristics of SpA and controls are shown in **Supplementary Table 3**. This study was approved by the institutional ethical committee of Ile-de-France XI (Saint-Germain-en-Laye France).

Analysis of Smad2/3 phosphorylation by flow cytometry. PBMC (10^6 cells/tube in PBS) from pairs of SpA patients and healthy controls were stimulated with recombinant human (rh) TGFβ (10 ng/mL; R&D Systems) or rhActivin A (20 ng/mL; R&D Systems) or not for 30 minutes at 37°C. After staining with anti-CD3 mAb (clone-UCHT1; BD Biosciences) and fixation during 20 minutes at 37°C with cytoFix Buffer (BD Biosciences), cells were permeabilized with perm buffer and stained with anti-p-Smad2 (pS465/pS467)/p-Smad3 (pS423/pS425) PhosFlow Ab according to the manufacturer's instructions (BD Biosciences) and analyzed using a LSRIII Fortessa flow cytometer (BD Biosciences). Results were expressed as staining index calculated as the ratio between samples and fluorescence-minus-one (FMO) staining control.

Western-blotting. Forty wing discs of third-instar larvae were dissected in PBS and crushed in 400µl of lysis buffer [Tris-HCl pH 8.2, 1M; NaCl 25mM; Nonidet P40 1% (NP40), protease inhibitor (complete Mini EDTA free, Roche, Boulogne-Billancourt, France)]. Total protein extract was completed by Laemmli 4X, DTT 0.5M and heated to 95°C for 5 minutes. Three independent samples of total protein were analyzed by Western-blot following a standard protocol, using rabbit anti-GRP78 (BiP) (ab21685, abcam),[19] HC-10, BBM1 and mouse anti-Lamin C (LC28.26, DSHB, Iowa, USA)[20] and peroxidase-conjugated goat anti-mouse Ig or rabbit Ig (Dakocytomation, Carpenteria, CA) for 1.5 hours. CD14-negative PBMC (1-2 10^6 cells) were lysed in lysis buffer [Tris-HCl pH 7.5

20mM; NaCl 20mM; Triton 100X 1%, EDTA 10mM, protease inhibitor (complete Mini EDTA free, Roche), phosphatase inhibitor (PhosSTOP, Roche, 04906837001), Na3VO4 [1mM]. 2 µg of proteins were separated in 4-12% gradient gel and transferred on a PVDF membrane. Blot was revealed following a standard protocol using rabbit anti-p-Smad2 (Cell Signaling #3108), rabbit anti-Smad2/3 (Cell Signaling #8685) and rabbit anti-Actin (Sigma #A2066).

Statistical analysis. Quantitative data are shown as the mean ± SEM. Unpaired Student's t-test was used for comparisons between two groups, unless otherwise stated. ANOVA was used for comparison of more than 2 groups, followed by unpaired Student's t-test after Bonferonni correction. Normality and homoscedasticity were respectively verified by Shapiro-Wilk and F tests before unpaired t-tests with n<30 or ANOVA. When data were not normal or homoscedastic, ANOVA was replaced by the Kruskal-Wallis test, followed by Dunn's multiple comparisons tests comparing each condition to the control. Wilcoxon matched-pairs test was used for comparison of matched groups. p values inferior to 0.05 were considered significant. The effect size was measured by Cohen's d.

Data availability. The authors declare that the main data supporting the findings of this study are available within the article and its Supplementary Information files.

Results

AS-associated *HLA-B27* alleles induce specific wing and eye phenotypes in *Drosophila*.

Transgenic flies, carrying SpA-associated *HLA-B*27:04* or *HLA-B*27:05* alleles in combination with *hβ2m* developed abnormal phenotypes. The adult fly wing contains five longitudinal veins (from the most anterior L1 to the posterior L5) spanning the length of the wing and the anterior (ACV) and posterior (PCV) crossveins that connect L3 to L4 and L4 to L5, respectively **(Fig. 1a)**. Neither expression of single transgenes **(Fig. 1b, c, e, g)**, nor expression of *HLA-B*07:02* with *hβ2m* **(Fig. 1d and Supplementary Fig. 1d)** induced any phenotype in the adult fly. However, expression of *HLA-B*27:04* or *HLA-B*27:05* with *hβ2m* induced a loss of ACV and/or PCV, when driven in the wing by *nub-GAL4* or *en-GAL4* **(Fig. 1f, h, and Supplementary Fig. 1d)**. Moreover, expression of *HLA-B27* alleles with *hβ2m* -but not of single transgenes nor of *HLA-B*07:02* with *hβ2m*- caused a significant reduction of the eye size, when driven by the eye-specific driver *ey-GAL4* **(Fig. 1i-l)**. We focused further studies on the crossveinless phenotype that was fully penetrant, in contrast to the eye phenotype.

The crossveinless phenotype is neither associated with ER stress nor cell death induction

Efficient MHC-I folding in the ER depends on the peptide-loading complex (PLC),[21] which lacks some components in *Drosophila*. Therefore, HLA-B*27:05/hβ2m expression in such organism could lead to ER stress and unfolded protein response (UPR), a mechanism that has been proposed to mediate HLA-B27 pathogenicity.[6] However, ER stress **(Supplementary Fig. 2a-c, 2f-g)** and apoptosis **(Supplementary Fig. 2h-j)** markers revealed no effect of HLA-B*27:05/hβ2m expression. Additionally, reducing putative ER stress **(Supplementary Fig. 2d-e)** or apoptosis **(Supplementary Fig. 2k-l)** did not modify the crossveinless phenotype, ruling out a role of ER stress or apoptosis in the HLA-B*27:05/hβ2m-induced phenotype.

***HLA-B*2705/hβ2m* expression misregulates BMP signaling**

Another hypothesis that may explain the crossveinless wings relies on the misregulation of the Notch, epidermal growth factor (EGF) or bone morphogenetic protein (BMP) pathways during

development.[22] Notch signaling is activated in the wing intervein cells and is required to prevent ectopic vein formation. Expression of *HLA-B*2705/hβ2m* transgenes in intervein cells under the control of *bs-GAL4* did not induce the crossveinless phenotype, whereas driving their expression in vein cells with *shv-GAL4* led to loss of ACV and PCV, arguing against involvement of Notch pathway (**Supplementary Fig. 3a-c**). To test if HLA-B*2705/hβ2m could interfere with EGF signaling, we quantified transcript levels of four EGF signaling target genes involved in wing development. None was modified, excluding the involvement of this pathway (**Supplementary Fig. 3d-g**).

The crossveinless wing phenotype induced by expression of HLA-B27/hβ2m in *Drosophila* phenocopies mutations of genes involved in BMP signaling.[23,24] During wing development, the BMP pathway induces the proveins position.[23,25,26] BMP signaling requires the formation of a hetero- or homodimer composed of the Decapentaplegic (Dpp) and/or Glass bottom boat (Gbb) ligands (**Fig. 2a**). Dimeric ligand binds to a heterotetramer composed of a hetero- or homodimer of BMP type I receptors (BMPR1, *i.e.* Thickveins (Tkv) and Saxophone (Sax)) and a hetero- or homodimer of the BMP type II receptors (BMPR2, *i.e.* Punt and Wishful thinking). Activated receptors phosphorylate the transcription factor Mad that associates with Medea for its import into the nucleus, where it induces transcription of *optomotor-blind* (*omb*), *spalt-major* (*spalm*), and *daughters against dpp* (*dad*).[25,26]

Expression of a dominant negative mutant of *gbb* or depletion of Dpp in the wing, resulted in a reduction of wing size and/or an alteration of venation, which were worse in the presence of HLA-B*27:05/hβ2m, demonstrating interaction between HLA-B*27:05/hβ2m and the BMP pathway (**Fig. 2b-e**). Overexpression of *gbb* or *dpp* induces the formation of a blistered wing (**Fig. 2f, h**). Interestingly, co-expression of HLA-B*27:05/hβ2m dramatically suppressed the *gbb* overexpression phenotype and reciprocally crossveins were restored by *gbb* overexpression (**Fig. 2g**). In contrast, co-expression of *HLA-B*27:05/hβ2m* suppressed very moderately the phenotype induced by *dpp* overexpression (**Fig. 2i**). These results showed that interaction between BMP signaling and HLA-B27 expression resulted in gbb-mediated signaling dampening.

*HLA-B*27:05/hβ2m* expression inhibits BMPR1 Sax function

To identify the level of interaction of HLA-B*27:05/hβ2m with the BMP signaling pathway, we tested the effect of HLA-B*27:05/hβ2m expression in a Mad-misregulated background. Interestingly, it had no significant effect on a constitutively active form of Mad (Mad.CA)-induced phenotype **(Fig. 2j, k)**, indicating that HLA-B27/hβ2m likely interacted upstream of the transcription factor Mad and potentially with BMP receptors. Since Gbb preferentially binds to Sax and Dpp to Tkv, we further investigated the interaction between HLA-B*27:05/hβ2m and Sax.[22,27] Sax can either promote BMP signaling by forming a heterodimer with Tkv, or, as a homodimer, limit the availability of Gbb and thereby antagonize signaling **(Fig. 3a)**.[28] Overexpression of a constitutively active form of *Sax* (*Sax.CA*) alters the formation of wings, which was suppressed by HLA-B*27:05/hβ2m, showing that *HLA-B*27:05/hβ2m* genetically repressed Sax activity **(Fig. 2l, m)**. As expected, if HLA-B*27:05/hβ2m repressed Sax, HLA-B*27:05/hβ2m had no effect on wing vein defects induced by a negative dominant mutant of *Sax* (*Sax.ΔI*) **(Fig. 2n, o)**.

Loss of function of *Sax* is known to widen the phosphorylated Mad (p-Mad) gradient, which results in an increase of its target genes expression.[28] Consistently, HLA-B*27:05/hβ2m behaved as Sax.ΔI: both induced a widening of pMad gradient in wing imaginal discs **(Fig. 4a-d)**. HLA-B*27:05/hβ2m also increased the transcript levels of BMP signaling targets *dad* and *omb* **(Fig. 4e-f)**. Altogether, those results supported an antagonistic interaction between HLA-B*27:05/hβ2m and Sax. The alternative hypothesis that HLA-B*27:05/hβ2m increased Tkv activity could be excluded, as genetic interaction between HLA-B*27:05/hβ2m and a constitutively active form of Tkv (Tkv.CA) decreased the phosphorylation of Mad and attenuated the Tkv.CA phenotype in adult wings **(Supplementary Fig. 4a-e)**. Suppression of Tkv.CA-induced phenotype by HLA-B*27:05/hβ2m is readily explained by HLA-B*27:05/hβ2m reducing Sax availability and the formation of Tkv-Sax heterodimers, thereby dampening BMP signaling **(Fig. 2b)**.

HLA-B*27:05 folds and localizes to the plasma membrane in *Drosophila*

HLA-B27 and HLA-B7 were previously observed at the surface of transfected *Drosophila* cells in a well-folded conformation and hβ2m-dependent manner.[29] Consistently, well-folded HLA-B*27:05 or HLA-B*07:02 were detected by immunostaining performed on wing imaginal discs using w6/32

and ME1 Abs, only when hβ2m was present **(Supplementary Fig. 5a-h and Supplementary 6a-d)**, indicating that hβ2m is essential to the HLA-B complex formation, as in mammals. Interestingly, HLA-B*27:05/hβ2m resulted in a more intense staining than HLA-B*07:02/hβ2m **(Supplementary Fig. 5a-h)**, albeit the amount of hβ2m in wing discs was similar between both conditions **(Supplementary Fig. 6e-g)**. Using flow cytometry on non-permeabilized cells from wing imaginal discs, we also detected a greater amount of well-folded HLA-B*27:05/hβ2m than HLA-B*07:02/hβ2m on the cell surface **(Supplementary Fig. 5i, j)**. Those results show that HLA-B*27:05 had a better folding capacity than HLA-B*07:02 when combined with hβ2m in the *Drosophila* context.

HLA-B*27:05 interacts with Sax in *Drosophila* and with ALK2 in AS patient's cells

We next investigated whether HLA-B*27:05/hβ2m and Sax could interact physically using PLA. Unlike the irrelevant human HA-tagged membrane protein hPen2-HA **(Fig. 5a, c)**, constitutively active HA-tagged Sax was indeed revealed in very close proximity (*i.e.* less than 40 nm) of HLA-B*27:05/hβ2m in the *Drosophila* wing imaginal disc, **(Fig. 5b, d)**. Moreover, the human Sax ortholog ALK2 and HLA-B27 were also found in close vicinity of each other at the surface of B-LCLs from AS patients. This interaction was specific for both proteins, since ALK2 neither co-localized with CD45, nor with any other HLA-B allotype **(Fig. 5e-k)**.

TGFβ superfamily ligands Activin A and TGFβ induce elevated Smad2/3 phosphorylation in T cells from HLA-B27+ SpA patients

ALK2, which is widely expressed in mammalian cells, binds several TGFβ superfamily ligands, including Activins and TGFβ and may antagonize their signaling that proceeds *via* Smad2/3 phosphorylation.[30–32] Thus, to determine if HLA-B27 would disturb TGFβ/BMP pathway signaling in SpA, we examined the phosphorylation of Smad2/3 in peripheral blood T lymphocytes from SpA patients **(Fig. 6)**. Indeed, we observed elevated phosphorylation of Smad2/3 in those cells, as compared to T cells from healthy controls. The difference was detectable in resting cells by PhosFlow but was exacerbated after exposure to TGFβ superfamily ligands (*i.e.* Activin A and TGFβ) consistent with a

repression of the antagonistic activity of ALK2 by HLA-B27, similar to its effect on Sax function in

Drosophila.

Discussion

We used *Drosophila* to uncover non-canonical effects that might underlie the as yet unexplained association of HLA-B27 with AS. Strikingly, flies transgenic for AS-associated HLA-B*27:04 and HLA-B*27:05, in combination with hβ2m, exhibited crossveinless and small-eye phenotypes. In contrast, co-expression of HLA-B*07:02 allele (which is known to be protective from AS)[33] with hβ2m, used as a control condition, did not affect fly development. These results underscore *HLA-B27*-expressing *Drosophila* as a new promising model to investigate HLA-B27 pathogenic effects, even if it bears some limitations owing to the lack of adaptive immune system.

In mammalian cells, HLA-B27 exhibits slow-folding capacity and a tendency to misfold, which was proposed as putative mechanism for its pathogenicity, by triggering ER stress and UPR.[6] This could have been the case in *Drosophila* that lacks tapasin and transporters associated with antigen processing, required for optimal folding of MHC-I molecules.[21] However, given that MHC-I misfolding is reduced in the presence of hβ2m,[34] and that neither expression of HLA-B alone nor its co-expression with hβ2m induced ER stress in transgenic *Drosophila*, it is unlikely that MHC-I misfolding would account for the observed phenotypes. Moreover, the level of folded HLA-B molecules at the cell surface was greater in HLA-B27/hβ2m than HLA-B7/hβ2m transgenic wing imaginal discs. Thus, well-folded conformers were likely responsible for the phenotypes occurring in flies co-expressing HLA-B27 and hβ2m.

In *Drosophila*, the formation of crossveins involves a cross-talk between BMP, EGF and Notch pathways.[22] To identify which pathway was implicated in the phenotype induced by HLA-B27/hβ2m, their alteration was systematically examined. BMP signaling disruption appeared to be primarily responsible for the crossveinless phenotype. Indeed, HLA-B27/hβ2m expression in the wing imaginal disc mimicked a Sax dominant negative mutant effect. BMP signaling balance in the wing was modified by HLA-B27/hβ2m, resulting in widening of p-Mad gradient and overall increased expression of p-Mad target genes, *i.e. omb* and *dad*, indicating a loss of the antagonistic function of Sax.[28] These results appear to be highly relevant to SpA as the BMP pathway also happens to be

misregulated in SpA patients. For instance, *Smad7* was up-regulated as its *Drosophila* ortholog *dad* in our model,[35]. Moreover, the p-Mad gradient widening seen in our model could fit with p-Smad1/5/8 detection in bony outgrowth of SpA patients, which is consistent with ectopic BMP signaling.[36] We interpreted this result by hypothesizing a repression of Sax function by the MHC-I molecule. Consistently, we showed that HLA-B27/hβ2m physically interacted with Sax in the wing tissue.

The mammalian orthologs of Sax are the BMPR1s ALK1 and ALK2, encoded by *ACVRL1* and *ACVR1* genes, respectively.[32] ALK1 is predominantly present on endothelial cells and involved in angiogenesis, whereas ALK2 is more widely expressed and exerts an essential role in cartilage development and endochondral ossification, particularly in the axial skeleton.[37,38] Both of them bind several TGFβ superfamily ligands, including BMPs, Activins and TGFβ, and like Sax, form hetero-tetrameric complexes with BMPR2s, including BMPRII and Activin receptor type-2A and -2B (ActRIIA and ActRIIB). [39,40]

Similar to Sax, ALK1 and 2 play either a positive or a negative role in signaling, depending on the ligand and BMPR2 binding. They transduce signal in response to BMPs via Smad1/5/8 phosphorylation, whereas they antagonize signaling mediated by Activin and TGFβ *via* Smad2/3 phosphorylation or even BMP-mediated signaling in some circumstances.[30–32,39,41–43] For instance, Activin A, is a ligand secreted by innate immune system cells during inflammation that primarily utilizes ALK4 and ALK7 as BMPR1s to initiate signaling via Smad2/3.[39,44,45] However, Activin A may also compete with BMPs to bind to ALK2, forming inactive complexes with ActRIIA and ActRIIB that inhibit Smad2/3-mediated Activin signaling and prevent Smad1/5/8-mediated BMP signaling.[31,46,47] Moreover, ALK2 can inhibit osteogenic BMP2- and BMP4-induced signaling by competing with their ALK3/ALK6 functional BMPR1s and recruiting BMPR2s into non-competent complexes.[41] Interestingly, loss of the inhibitory effect of ALK2 on BMP signaling in response to Activin A, due to mutations in *ACVR1* gene, leads to fibrodysplasia ossificans progressiva, a rare genetic disorder characterized by episodic heterotopic ossification of soft connective tissue, including tendons, ligaments, fascia, that may sometime bear similarities with AS.[48–51]

Interestingly, when expressed in *Drosophila*, ALK2 inhibited endogenous BMP signaling in wing discs like Sax did, suggesting that HLA-B27/hβ2m may interfere with ALK2 in mammals in a way similar to Sax in *Drosophila*.[32] Indeed, we observed that well-folded HLA-B27/hβ2m physically interacted with ALK2 at the surface of B-LCLs from AS patients and that this was not the case for the non-AS-associated HLA-B7 or HLA-B22 alleles that were also recognized by ME1 Ab. Characteristics of HLA-B27 explaining specific interaction with BMPR1s Sax/ALK2 remain to be determined. Interestingly however, one of the distinctive features common to all HLA-B27 alleles is an unpaired free cystein at position 67 that could potentially interact with the cystein-rich extra-cellular binding domain of Sax and ALK2 [52]

This prompted us to examine whether the presence of HLA-B27 would affect the response of immune cells from SpA patients to Activin A and TGFβ, two ligands known to bind ALK2 and that could be implicated in the disease process. Most interestingly, as predicted if the presence of HLA-B27/hβ2m released a brake on Activin A/TGFβ signaling, we observed elevated Smad2/3 phosphorylation that was detected in resting cells and exacerbated in response to both ligands in T cells from SpA patients.

Based on our findings, we propose a mechanism for HLA-B27 implication in SpA, whereby HLA-B27/hβ2m antagonizing the inhibitory function of ALK2 would potentiate Activin A, TGFβ, and/or BMP signaling in context-dependent fashion. A shift towards Smad2/3-mediated signaling in a context of inflammatory stimulus could notably contribute to the T-helper 17 differentiation bias[53] that has been shown in SpA.[6,54] Complementarily, release of the brake normally held by ALK2 on BMP-mediated endochondral ossification, in inflammatory context, could account for increased ossification, which is another striking hallmark of SpA - albeit this study does not address other factors that may contribute to AS in HLA-B27-negative cases.[55,56] This fits one of the oldest hypotheses proposed to account for HLA-B27 pathogenicity, i.e. that HLA-B27 itself might confer an enhanced sensitivity to an inflammatory mediator [57].

Acknowledgments and affiliations

Author Information: The authors declare no competing financial interests. Correspondence and requests for materials should be addressed to M.B. (maxime.breban@aphp.fr).

Patient and Public Involvement statement: We did not involve patients or the public in our work

References

1   Taurog JD, Chhabra A, Colbert RA. Ankylosing Spondylitis and Axial Spondyloarthritis. *N Engl J Med* 2016;**375**:1303. doi:10.1056/NEJMc1609622

2   Caffrey MFP, James DCO. Human Lymphocyte Antigen Association in Ankylosing Spondylitis. *Nature* 1973;**242**:121–121. doi:10.1038/242121a0

3   Rock KL, Reits E, Neefjes J. Present Yourself! By MHC Class I and MHC Class II Molecules. *Trends Immunol* 2016;**37**:724–37. doi:10.1016/j.it.2016.08.010

4   Bowness P. HLA-B27. *Annu Rev Immunol* 2015;**33**:29–48. doi:10.1146/annurev-immunol-032414-112110

5   Benjamin RJ, Madrigal JA, Parham P. Peptide binding to empty HLA-B27 molecules of viable human cells. *Nature* 1991;**351**:74–7. doi:10.1038/351074a0

6   Colbert RA, Tran TM, Layh-Schmitt G. HLA-B27 misfolding and ankylosing spondylitis. *Mol Immunol* 2014;**57**:44–51. doi:10.1016/j.molimm.2013.07.013

7   Chao H-T, Liu L, Bellen HJ. Building dialogues between clinical and biomedical research through cross-species collaborations. *Sem Cell Dev Biol* 2017;**70**:49–57. doi:10.1016/j.semcdb.2017.05.022

8   Brand AH, Perrimon N. Targeted gene expression as a means of altering cell fates and generating dominant phenotypes. *Development* 1993;**118**:401–15.

9   Jeanty C, Sourisce A, Noteuil A, *et al.* HLA-B27 subtype oligomerization and intracellular accumulation patterns correlate with predisposition to spondyloarthritis. *Arthritis Rheumatol* 2014;**66**:2113–23. doi:10.1002/art.38644

10   Demay Y, Perochon J, Szuplewski S, *et al.* The PERK pathway independently triggers apoptosis and a Rac1/Slpr/JNK/Dilp8 signaling favoring tissue homeostasis in a chronic ER stress Drosophila model. *Cell Death Dis* 2014;**5**:e1452. doi:10.1038/cddis.2014.403

11   Florentin A, Arama E. Caspase levels and execution efficiencies determine the apoptotic potential of the cell. *J Cell Biol* 2012;**196**:513–27. doi:10.1083/jcb.201107133

12   Wong JT, Akhbar F, Ng AYE, *et al.* DIP1 modulates stem cell homeostasis in Drosophila through regulation of sisR-1. *Nat Commun* 2017;**8**:759. doi:10.1038/s41467-017-00684-4

13   Stam NJ, Spits H, Ploegh HL. Monoclonal antibodies raised against denatured HLA-B locus heavy chains permit biochemical characterization of certain HLA-C locus products. *J Immunol* 1986;**137**:2299–306.

14   Ellis SA, Taylor C, McMichael A. Recognition of HLA-B27 and related antigen by a monoclonal antibody. *Hum Immunol* 1982;**5**:49–59.

15   Barnstable CJ, Bodmer WF, Brown G, *et al.* Production of monoclonal antibodies to group A erythrocytes, HLA and other human cell surface antigens-new tools for genetic analysis. *Cell* 1978;**14**:9–20.

16   Brodsky FM, Parham P. Monomorphic anti-HLA-A,B,C monoclonal antibodies detecting molecular subunits and combinatorial determinants. *J Immunol* 1982;**128**:129–35.

17   Costantino F, Talpin A, Evnouchidou I, *et al.* ERAP1 Gene Expression Is Influenced by Nonsynonymous Polymorphisms Associated With Predisposition to Spondyloarthritis. *Arthritis Rheumatol* 2015;**67**:1525–34. doi:10.1002/art.39072

18   Martín-Esteban A, Guasp P, Barnea E, *et al.* Functional Interaction of the Ankylosing Spondylitis-Associated Endoplasmic Reticulum Aminopeptidase 2 With the HLA-B*27 Peptidome in Human Cells: ERAP-2 and the HLA-B*27 Peptidome. *Arthritis Rheumatol* 2016;**68**:2466–75. doi:10.1002/art.39734

19   Sanchez-Martinez A, Beavan M, Gegg ME, *et al.* Parkinson disease-linked GBA mutation effects reversed by molecular chaperones in human cell and fly models. *Sci Rep* 2016;**6**:31380. doi:10.1038/srep31380

20   Schulze SR, Curio-Penny B, Li Y, *et al.* Molecular genetic analysis of the nested Drosophila melanogaster lamin C gene. *Genetics* 2005;**171**:185–96. doi:10.1534/genetics.105.043208

21   Blees A, Januliene D, Hofmann T, *et al.* Structure of the human MHC-I peptide-loading complex. *Nature* 2017;**551**:525–8. doi:10.1038/nature24627

22   Sotillos S, De Celis JF. Interactions between the Notch, EGFR, and decapentaplegic signaling pathways regulate vein differentiation duringDrosophila pupal wing development. *Dev Dyn* 2005;**232**:738–52. doi:10.1002/dvdy.20270

23   Ralston A, Blair SS. Long-range Dpp signaling is regulated to restrict BMP signaling to a crossvein competent zone. *Dev Biol* 2005;**280**:187–200. doi:10.1016/j.ydbio.2005.01.018

24   Matsuda S, Yoshiyama N, Künnapuu-Vulli J, *et al.* Dpp/BMP transport mechanism is required for wing venation in the sawfly Athalia rosae. *Insect Biochem Mol Biol* 2013;**43**:466–73. doi:10.1016/j.ibmb.2013.02.008

25   Crozatier M, Glise B, Vincent A. Patterns in evolution: veins of the Drosophila wing. *Trends Genet* 2004;**20**:498–505. doi:10.1016/j.tig.2004.07.013

26   Raftery LA, Umulis DM. Regulation of BMP activity and range in Drosophila wing development. *Curr Opin Cell Biol* 2012;**24**:158–65. doi:10.1016/j.ceb.2011.11.004

27   Haerry TE. The interaction between two TGF-beta type I receptors plays important roles in ligand binding, SMAD activation, and gradient formation. *Mech Dev* 2010;**127**:358–70. doi:10.1016/j.mod.2010.04.001

28   Bangi E. Dual function of the Drosophila Alk1/Alk2 ortholog Saxophone shapes the Bmp activity gradient in the wing imaginal disc. *Development* 2006;**133**:3295–303. doi:10.1242/dev.02513

29   Jackson MR, Song ES, Yang Y, *et al.* Empty and peptide-containing conformers of class I major histocompatibility complex molecules expressed in Drosophila melanogaster cells. *Proc Natl Acad Sci USA* 1992;**89**:12117–21.

30   Oh SP, Seki T, Goss KA, *et al.* Activin receptor-like kinase 1 modulates transforming growth factor-beta 1 signaling in the regulation of angiogenesis. *Proc Natl Acad Sci USA* 2000;**97**:2626–31.

31   Renlund N, O'Neill FH, Zhang L, *et al.* Activin receptor-like kinase-2 inhibits activin signaling by blocking the binding of activin to its type II receptor. *J Endocrinol* 2007;**195**:95–103. doi:10.1677/JOE-07-0281

32   Le V, Anderson E, Akiyama T, *et al.* Drosophila models of FOP provide mechanistic insight. *Bone* 2018;**109**:192–200. doi:10.1016/j.bone.2017.11.001

33   Costantino F, Breban M, Garchon H-J. Genetics and Functional Genomics of Spondyloarthritis. *Front Immunol* 2018;**9**:2933. doi:10.3389/fimmu.2018.02933

34   Tran TM, Dorris ML, Satumtira N, *et al.* Additional human β2-microglobulin curbs HLA–B27 misfolding and promotes arthritis and spondylitis without colitis in male HLA–B27–transgenic rats. *Arthritis Rheum* 2006;**54**:1317–27. doi:10.1002/art.21740

35   Lee YH, Song GG. Meta-analysis of differentially expressed genes in ankylosing spondylitis. *Genet Mol Res* 2015;**14**:5161–70. doi:10.4238/2015.May.18.6

36   Lories RJU, Derese I, Luyten FP. Modulation of bone morphogenetic protein signaling inhibits the onset and progression of ankylosing enthesitis. *J Clin Invest* 2005;**115**:1571–9. doi:10.1172/JCI23738

37   Salazar VS, Gamer LW, Rosen V. BMP signalling in skeletal development, disease and repair. *Nat Rev Endocrinol* 2016;**12**:203–21. doi:10.1038/nrendo.2016.12

38   Roman BL, Hinck AP. ALK1 signaling in development and disease: new paradigms. *Cell Mol Life Sci* 2017;**74**:4539–60. doi:10.1007/s00018-017-2636-4

39   Yadin D, Knaus P, Mueller TD. Structural insights into BMP receptors: Specificity, activation and inhibition. *Cytokine Growth Factor Rev* 2016;**27**:13–34. doi:10.1016/j.cytogfr.2015.11.005

40   ten Dijke P, Yamashita H, Ichijo H, *et al.* Characterization of type I receptors for transforming growth factor-beta and activin. *Science* 1994;**264**:101–4.

41   Hildebrand L, Stange K, Deichsel A, *et al.* The Fibrodysplasia Ossificans Progressiva (FOP) mutation p.R206H in ACVR1 confers an altered ligand response. *Cell Signal* 2017;**29**:23–30. doi:10.1016/j.cellsig.2016.10.001

42   Goumans MJ, Valdimarsdottir G, Itoh S, *et al.* Activin receptor-like kinase (ALK)1 is an antagonistic mediator of lateral TGFbeta/ALK5 signaling. *Mol Cell* 2003;**12**:817–28.

43   Ebner R, Chen R, Shum L, *et al.* Cloning of a type I TGF-beta receptor and its effect on TGF-beta binding to the type II receptor. *Science* 1993;**260**:1344–8. doi:10.1126/science.8388127

44   Phillips DJ, de Kretser DM, Hedger MP. Activin and related proteins in inflammation: not just interested bystanders. *Cytokine Growth Factor Rev* 2009;**20**:153–64. doi:10.1016/j.cytogfr.2009.02.007

45   de Kretser DM, O'Hehir RE, Hardy CL, *et al.* The roles of activin A and its binding protein, follistatin, in inflammation and tissue repair. *Mol Cell Endocrinol* 2012;**359**:101–6. doi:10.1016/j.mce.2011.10.009

46   Alessi Wolken DM, Idone V, Hatsell SJ, *et al.* The obligatory role of Activin A in the formation of heterotopic bone in Fibrodysplasia Ossificans Progressiva. *Bone* 2018;**109**:210–7. doi:10.1016/j.bone.2017.06.011

47   Olsen OE, Wader KF, Hella H, *et al.* Activin A inhibits BMP-signaling by binding ACVR2A and ACVR2B. *Cell Commun Signal* 2015;**13**:27. doi:10.1186/s12964-015-0104-z

48   Fukuda T, Kohda M, Kanomata K, *et al.* Constitutively Activated ALK2 and Increased SMAD1/5 Cooperatively Induce Bone Morphogenetic Protein Signaling in Fibrodysplasia Ossificans Progressiva. *J Biol Chem* 2009;**284**:7149–56. doi:10.1074/jbc.M801681200

49   Shore EM, Xu M, Feldman GJ, *et al.* A recurrent mutation in the BMP type I receptor ACVR1 causes inherited and sporadic fibrodysplasia ossificans progressiva. *Nat Genet* 2006;**38**:525–7. doi:10.1038/ng1783

50   Bridges AJ, Hsu KC, Singh A, *et al.* Fibrodysplasia (myositis) ossificans progressiva. *Semin Arthritis Rheum* 1994;**24**:155–64.

51   Dugar M, Limaye V, Cleland LG, *et al.* Fibrodysplasia ossificans progressiva presenting as ankylosing spondylitis. *Intern Med J* 2010;**40**:862–4. doi:10.1111/j.1445-5994.2010.02363.x

52   Massagué J. TGF-β signal transduction. *Annu Rev Biochem* 1998;**67**:753–91. doi:10.1146/annurev.biochem.67.1.753

53   Zhang S. The role of transforming growth factor β in T helper 17 differentiation. *Immunology* 2018;**155**:24–35. doi:10.1111/imm.12938

54   Glatigny S, Fert I, Blaton MA, *et al.* Proinflammatory Th17 cells are expanded and induced by dendritic cells in spondylarthritis-prone HLA-B27-transgenic rats. *Arthritis Rheum* 2012;**64**:110–20. doi:10.1002/art.33321

55   Bennett AN, McGonagle D, O'Connor P, *et al.* Severity of baseline magnetic resonance imaging-evident sacroiliitis and HLA-B27 status in early inflammatory back pain predict radiographically evident ankylosing spondylitis at eight years. *Arthritis Rheum* 2008;**58**:3413–8. doi:10.1002/art.24024

56   Dougados M, Sepriano A, Molto A, *et al.* Sacroiliac radiographic progression in recent onset axial spondyloarthritis: the 5-year data of the DESIR cohort. *Ann Rheum Dis* 2017;**76**:1823–8. doi:10.1136/annrheumdis-2017-211596

57   Rosenbaum JT. Why HLA-B27: an analysis based on two animal models. *Ann Intern Med* 1981;**94**:261–3. doi:10.7326/0003-4819-94-2-261

Figures legend

Figure 1. Specific crosssveinless and small-eye phenotypes in *Drosophila* co-expressing AS-associated *HLA-B27* with *hβ2m*. (a-h) *nub-GAL4* was used to drive transgenes expression in the wing. Scale bar: 200 μm. Wild-type (WT) adult wing **(a)** and wings of flies expressing *hβ2m* alone (*nub-GAL4/+; UAS-hβ2m/+*) **(b)**, non-AS-associated *HLA-B*07:02* (*nub-GAL4/+; UAS-HLA-B*07:02/+* and *nub-GAL4/+; UAS-HLA-B*07:02,UAS-hβ2m/+*) **(c, d)**, AS-associated *HLA-B*27:04* (*nub-GAL4/+; UAS-HLA-B*27:04/+* and *nub-GAL4/+; UAS-HLA-B*27:04,UAS-hβ2m/+*) **(e, f)**, AS-associated *HLA-B*27:05* (*nub-GAL4/+; UAS-HLA-B*27:05/+* and *nub-GAL4/+; UAS-HLA-B*27:05,UAS-hβ2m/+*) **(g, h)** alone **(c, e, g)** or together with *hβ2m* **(d, f, h)**. Co-expression of *HLA-B*27:04* **(f)** or *HLA-B*27:05* **(h)** with *hβ2m* transgenes resulted in the complete or partial disappearance of both crossveins (arrows). **(i-k)** *ey-GAL4* was used to drive transgenes expression in the eye. Scale bar: 200 μm. Eye aspect of an *ey-GAL4/+* control **(i)**. Eye co-expressing *HLA-B*07:02* **(j)** or *HLA-B*27:05* **(k)** with *hβ2m*, the latest showing a reduced size. **(l)** Quantification of male *Drosophila* eye size (red box indicates flies expressing both an AS-associated *HLA-B27* allele and *hβ2m*). Box-and-whiskers graphs show the median, range and interquartile range of the data; Kruskal-Wallis: $p<10^{-4}$, followed by Dunn's multiple comparisons test showing significant difference with the control, only for *B*27:04/hβ2m* and *B*27:05/hβ2m* ($p<10^{-4}$ for both comparisons).

Figure 2. HLA-B27:05/hβ2m genetically interacts with BMP signaling components in *Drosophila* wings. (a) Schematic representation of BMP signaling pathway components (i.e. ligands, BMPR1s, transcription factor and target genes) in *Drosophila* (bold) and their corresponding orthologs in human. **(b)** Overexpression of a loss-of-function mutant targeting the cleavage site of *gbb* induces a crossveinless phenotype and a partial loss of posterior longitudinal veins (*nub/+; UAS-gbb.R126A.R325A.K334N/+*). **(c)** Genetic interaction with HLA-B*27:05/hβ2m further deletes the longitudinal wing veins (*nub/+; UAS-gbb.R126A.R325A.K334N/UAS-HLA-B*27:05,UAS-hβ2m*). **(d)** Depletion of Dpp results in a reduction of wing size and the absence of wing venation (*nub/+; UAS-RNAi-dpp/+*). Scale bar: 200μm. **(e)** Genetic interaction with HLA-B*27:05/hβ2m worsens Dpp-

depletion phenotype (*nub/+; UAS-RNAi-dpp/UAS-HLA-B*27:05,UAS-hβ2m*). **(f)** Overexpression of *gbb* results in a blistered and pigmented adult wing (*nub-GAL4/+; UAS-gbb/+*). **(g)** Genetic interaction between HLA-B*27:05/hβ2m and *gbb* overexpression results in suppression of *gbb-* and HLA-B*27:05/hβ2m-induced phenotypes (*nub-GAL4/+; UAS-gbb/UAS-HLA-B*27:05,UAS-hβ2m*). **(h)** Overexpression of *dpp* phenocopies *gbb* overexpression (*nub-GAL4/+; UAS-dpp/+*). **(i)** Genetic interaction with HLA-B*27:05/hβ2m, reverses only partially Dpp-induced phenotype (*nub-GAL4/+; UAS-dpp/UAS-HLA-B*27:05,UAS-hβ2m*). **(j)** Overexpression of a constitutively active form of Mad induces extravein formation *(nub/+; UAS-Mad.CA/+)*. **(k)** HLA-B*27:05/hβ2m does not significantly modify the extravein phenotype (*nub/+; UAS-Mad.CA/UAS-HLA-B*27:05,UAS-hβ2m*). **(l)** A constitutively active form of Sax provokes minor vein defects and blisters (*nub-GAL4/+; UAS-sax.CA/+*). **(m)** Genetic interaction with HLA-B*27:05/hβ2m partially suppresses this phenotype (*nub-GAL4/+; UAS-sax.CA/UAS-HLA-B*27:05,UAS-hβ2m*). **(n)** Expression of a Sax depleted of its kinase domain results in a narrowed adult wing with defects in the formation of L2 and L5 veins (*nub-GAL4/+; UAS-saxΔI/+*). **(o)** Genetic interaction with HLA-B*27:05/hβ2m does not modify the SaxΔI-induced phenotype (*nub-GAL4/+; UAS-saxΔI/UAS-HLA-B*27:05,UAS-hβ2m*).

Figure 3. Proposed model of interaction between HLA-B*27:05/hβ2m and the BMP pathway. Representation of *Drosophila* BMP signaling pathway in wild type cells **(a)** and in HLA-B*27:05/hβ2m-expressing cells **(b)** of wing imaginal discs. Three different forms of BMPR1 dimers exist: Tkv-Tkv and Sax-Sax homodimers, and Tkv-Sax heterodimers. Gbb (blue) and Dpp (green) ligands of the BMP pathway show distinct binding preferences. Thicker arrows indicate preponderant signaling because of ligand and receptor availability as well as affinity differences. Signaling in the cells close to the antero-posterior frontier (A-P axis) is shown on the left, signaling in the cells distant from this frontier is represented on the right. **(a)** The Tkv-Sax heterodimeric receptor is the main complex that mediates BMP signaling. Tkv-Tkv homodimers also activate BMP signaling but less. Sax-Sax homodimers do not activate BMP signaling but limit the range of Gbb diffusion, restricting p-Mad gradient from the A-P frontier. *omb* (purple) and *dad* (orange) are target genes of BMP

signaling. **(b)** Ectopic HLA-B*27:05/hβ2m in the wing pouch induces a widening of p-Mad gradient, resulting in an increase of *omb* and *dad* expressing cells. We show that HLA-B*27:05/hβ2m interacts with Sax, which may reduce Sax-Sax homodimer and Tkv-Sax heterodimer formation (pale blue Sax). Sax receptor sequestration by HLA-B*27:05/hβ2m would result in an expansion of the Gbb gradient, disrupting BMP signaling.

Figure 4. HLA-B27:05/hβ2m misregulates BMP signaling similar to a *Sax* loss of function. (a-c) Projections from confocal stacks of third-instar larval wing imaginal discs stained with an anti-p-Mad antibody of wild-type (WT) **(a)**, *nub-GAL4/+; UAS-saxΔI* **(b)** and *nub-GAL4/+; UAS-HLA-B*27:05,UAS-hβ2m/+* **(c)** discs. Scale bar: 200 μm. **(d)** Quantification of p-Mad staining reported to imaginal discs width in the foregoing genotypes. Box-and-whiskers graphs show the median, range and interquartile range of the data; the p-values correspond to Dunn's multiple comparisons test following significant Kruskal-Wallis test. **(e,f)** Quantification of *dad* and *omb* transcripts expression (three independent experiments; the p values of paired t-tests are shown; *dad*: Cohen's d=8.17 and *omb*: Cohen's d=1.94).

Figure 5. HLA-B27 interacts with Sax and ALK2. (a-d) PLA performed with w6/32 and anti-HA Abs on the wing pouch cells expressing HLA-B*27:05/hβ2m and HA-tagged-hPen2 (negative control) **(a, c)** or HLA-B*27:05/hβ2m and HA-tagged Sax.CA with nub-GAL4 driver **(b, d)**. **(e-h)** PLA conducted in B-LCL *10151* from an HLA-B*27:05/B*15 AS patient with w6/32 and either anti-CD45 (negative control) **(e, g)** or anti-ALK2 Abs **(f, h)**. **c**, **d**, **g** and **h** are zoomed in details of boxed areas from **a**, **b**, **e** and **f**, respectively. **(i-j)** PLA conducted on B-LCLs *9435* from an HLA-B*7/B*44 healthy control **(i)** or *6370* from an HLA-B*27:05/B*44 AS patient **(j)** with ME1 and anti-ALK2 antibodies. **(k)** Average number of PLA staining dots/cell showing an interaction between ALK2 and HLA-A/B/C (ALK2-w6/32) or HLA-B*27/B*7/B*22 (ALK2-ME1) in B-LCLs from 3 controls and 3 AS patients. No signal was detected with ALK2, ME1 or w6/32 antibodies alone. Ten random 40x images per condition were acquired using the DAPI (grey nuclei) and Cy5 (white PLA signals) filters. Two-way ANOVA (factors: Ab and cell line) followed by Bonferroni's multiple-comparisons test: $p < 10^{-4}$.

Figure 6. p-Smad2/3 is increased in immune cells from HLA-B27+ SpA patients in response to Activin A or TGFβ. (a) Intracellular p-Smad2/3 was quantified in T cells from paired HLA-B27+ SpA patients and HLA-B27 negative healthy controls, after exposure to PBS, Activin A or TGFβ. Left: representative expression histograms. Right: scatter graph of staining index calculated as the ratio between samples and fluorescence-minus-one (FMO). Similar symbols indicate paired conditions. Horizontal bars show the mean values (12-16 independent experiments). Of note, statistical analysis performed after excluding the 3 case-control pairs corresponding to the most extreme outliers from the SpA group yielded significant p-values (PBS: p=0.01; Activin: P=0.012; TGFβ: p=0.002). (**b**) Western-blot showing p-Smad2, Smad2 and Smad3 in CD14-negative PBMC from HLA-B27 negative control and HLA-B27+ SpA patients. Values beneath the blots indicate the relative intensity of p-Smad2/Smad2 bands (representative of 2 independent experiments).
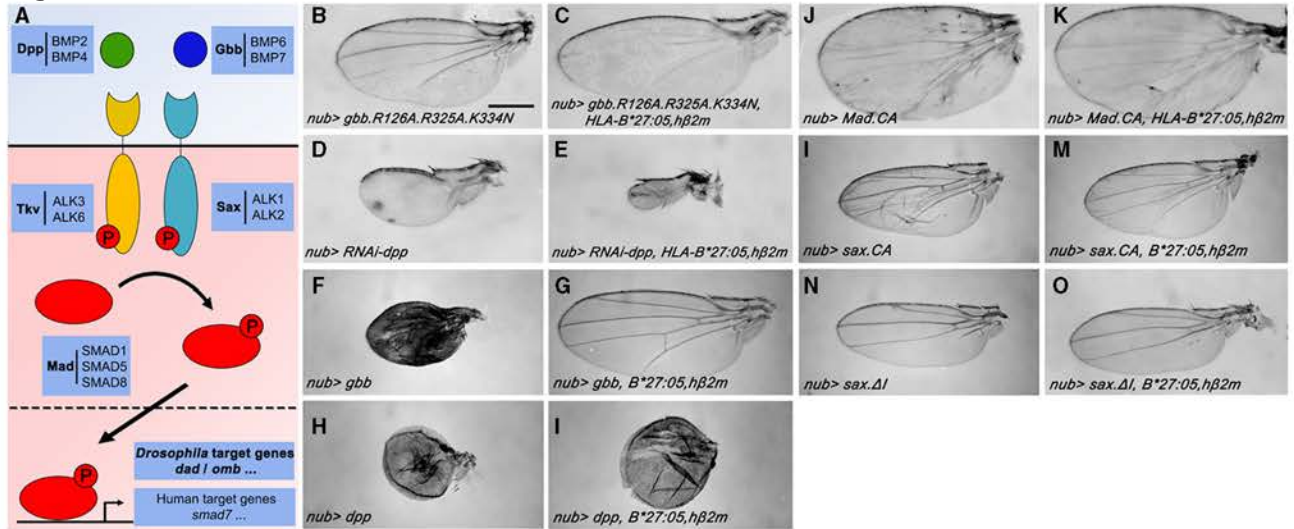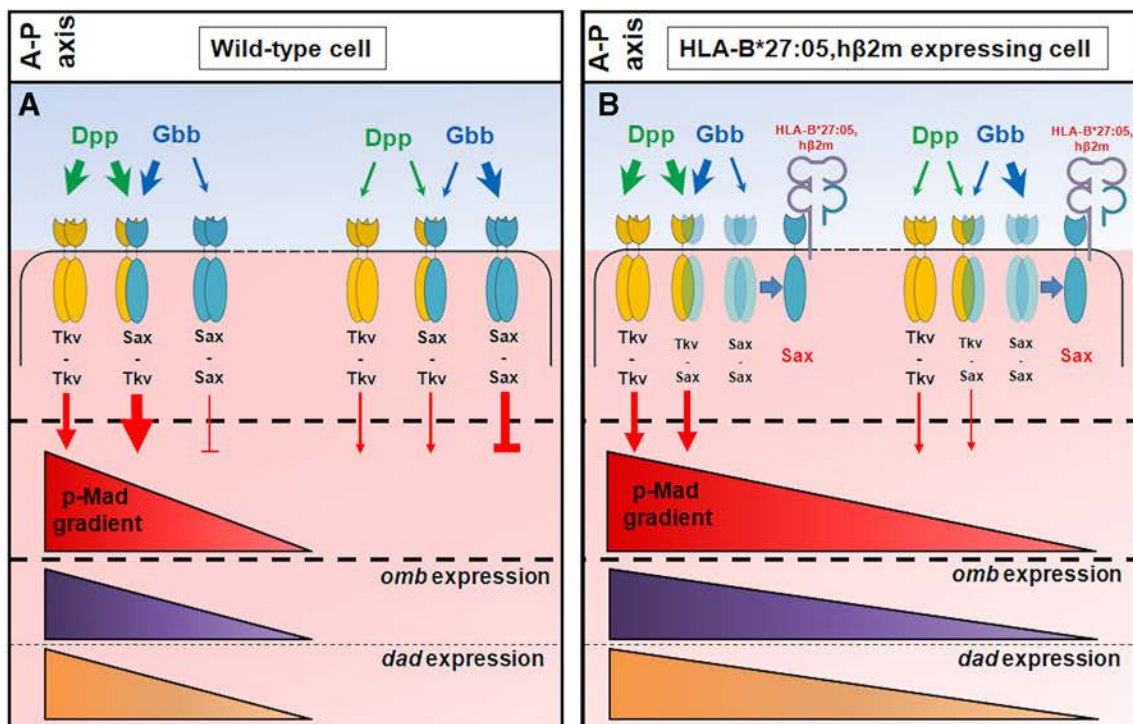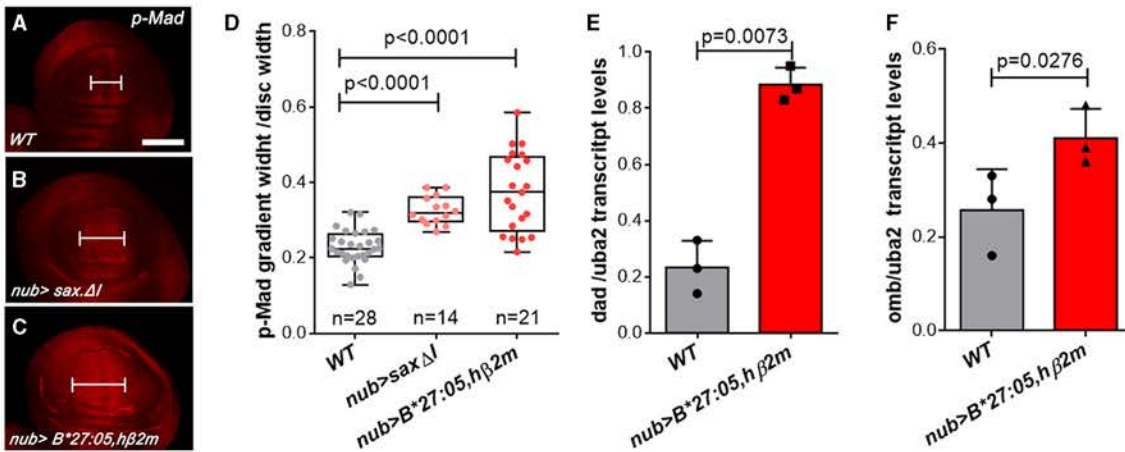
Figure 1
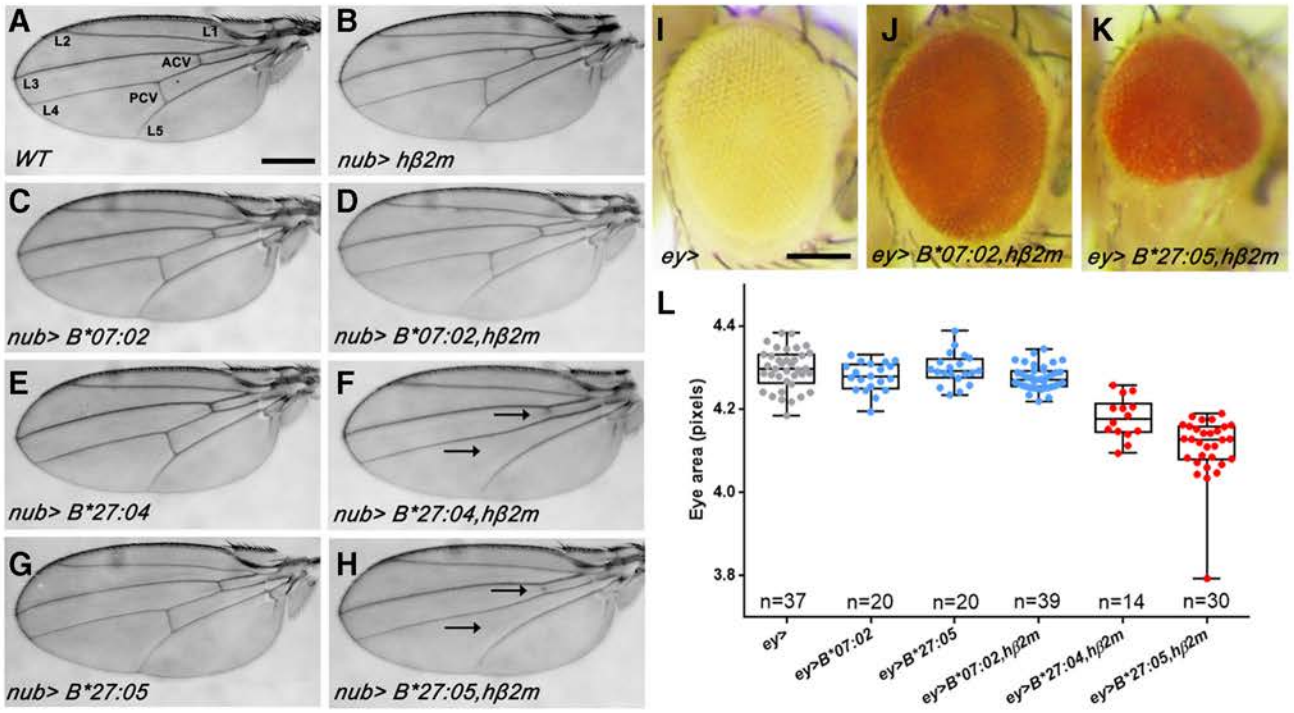
Figure 2

Figure 3

Figure 4

Figure 5
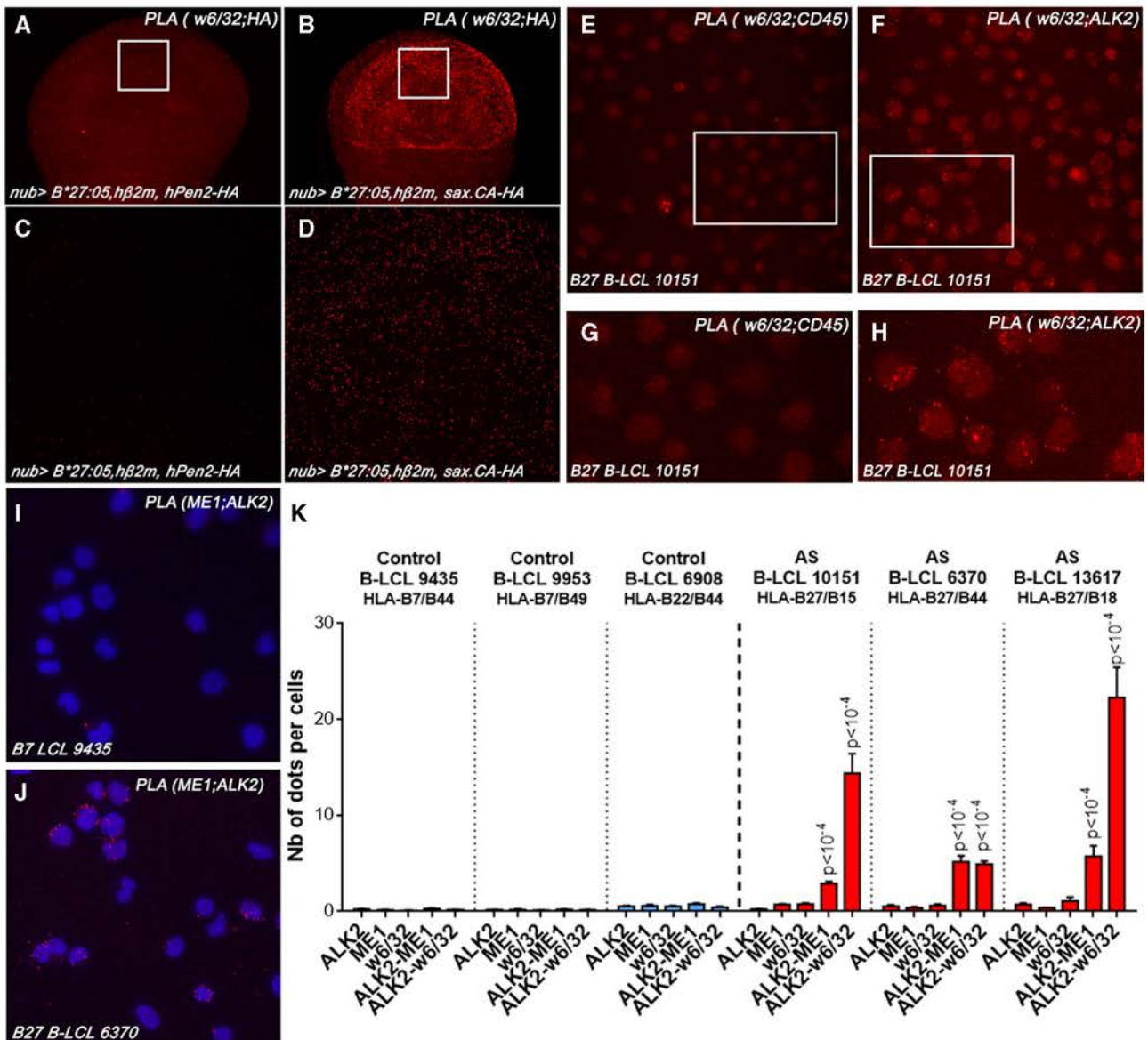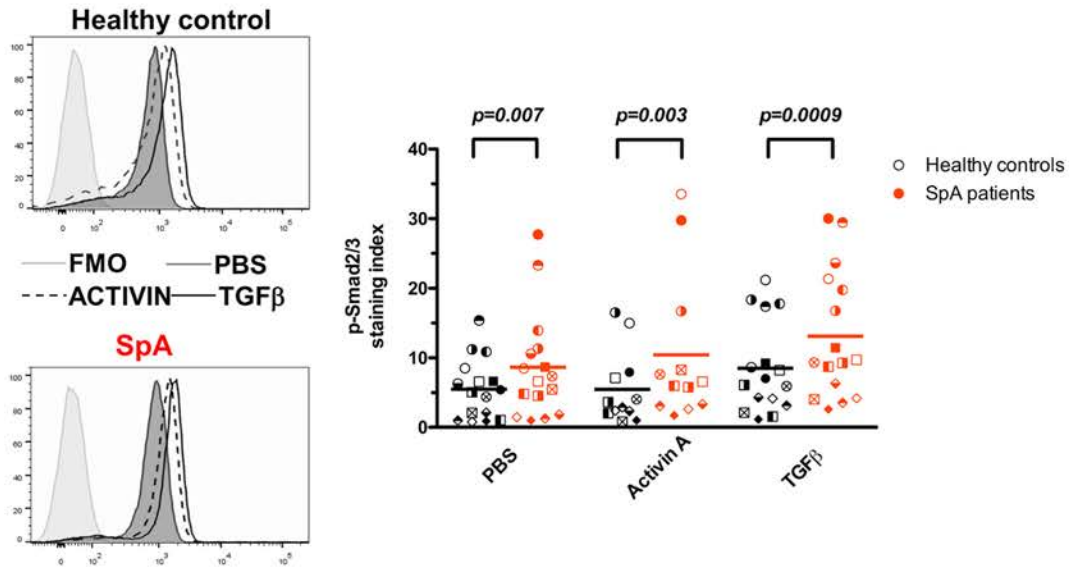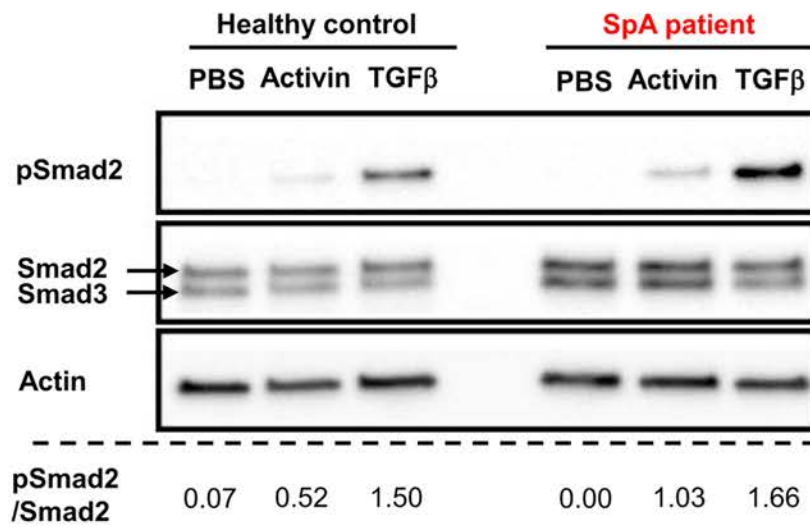
Figure 6

Supplementary Table 1. List of drivers and *Drosophila* lines used in the study.

Fly ID (short-hand name)	Genotype	Description	Bloomington stock # /Donor	Reference
Control fly strain				
white (w¹¹¹⁸)	w1118		Lab stock	N/A
Driver fly strain				
nubbin (nub-GAL4)	w*; P{nub-GAL4.K}2/CyoGFP;Dr/TM6b	Drives expression in the central portion of the discs, including the wing and haltere pouches	Lab stock	[1]
engrailed (en-GAL4)	y1 w*; P{en2.4-GAL4}e16E	Drives expression throughout development in posterior compartments	#30564	[2]
eyeless (ey-GAL4)	w*; P{GAL4-ey.H}3-8	Drives expression throughout the eye disc beginning before the stage of furrow initiation	#5534	[3]
blistered (bs-GAL4)	w*; P{GAL4}bs1348	Drives expression in pupal intervein regions	#6354	[4]
shortvein (shv ³ᴷᴾᴺ-GAL4)		Drives expression preferentially in the longitudinal veins L2, L3, L4, and distal L5 from at least 14 hr APF until at least 40 hr APF	De Celis Lab	[5]
loss-of-function mutation, or overexpressing wild type or mutant alleles				
rhodopsin/ninaE (UAS-Rh1G69D)	w*; ninaEG69D/TM6B, Tb1	Aggregate-prone mutant rhodopsin overexpression	#64123	[6]
X-box binding protein 1 (UAS-xbp1::EGFP)	w1118; PBac{Xbp1-GFP.FPTB}VK00033	ER stress (xbp1) reporter	#67735	[6]
heat shock 70-kDa protein cognate 3 (UAS-BiP)	y 1 w67c23 P{EPgy2}Hsc70-3EY11233	hsc70-3 overexpression	#20668	N/A
p35 (UAS-p35)	P{UAS-p35.H}BH3, w*	p35 overexpression	#6298	[7]
glass bottom boat (UAS-gbb.GFP)	y 1 w*; P{UASp-gbb.GFP}33.1	gbb overexpression	#63058	N/A
decapentaplegic (UAS-dpp.S)	w*; P{UAS-dpp.S}42B.4	dpp overexpression	#1486	[8]
decapentaplegic (UAS-dpp-RNAi)	y 1 v1; P{TRiP.JF01371}attP2	dpp loss-of-function	#25782	[9]
glass bottom boat (UAS-gbb. R126A.R325A.K334N)	y 1 w*; P{UAS-gbb.R126A.R325A.K334N}86b/ TM3, Sb1 Ser1	gbb loss-of-function	#63059	[10]
thickveins (UAS-tkv.CA)	w*; P{UAS-tkv.CA}3	Constitutively active form of tkv overexpression	#36537	[11]
presenilin enhancer 2 homolog (UAS-hPEN2.HA)	y 1 w*; M{UAS-hPSENEN.HA}ZH-86Fb	hPEN2 overexpression	#65759	[12]
mothers against dpp (UAS-mad.SDVD)		Constitutively active form of mad overexpression	De Celis Lab	[13]
saxophone (UAS-sax.Q263D.HA)		Constitutively active form of sax overexpression	Newfeld Lab	[13]
saxophone (UAS-saxΔI)		sax loss-of-function	Newfeld Lab	[14]

1. Kambadur R, Koizumi K, Stivers C, Nagle J, Poole SJ, Odenwald WF (1998) Regulation of POU genes by castor and hunchback establishes layered compartments in the Drosophila CNS. Genes & Development 12:246–260

2. Johnson RL, Grenier JK, Scott MP (1995) patched overexpression alters wing disc size and pattern: transcriptional and post-transcriptional effects on hedgehog targets. Development 121:4161–4170

3. Hazelett DJ, Bourouis M, Walldorf U, Treisman JE (1998) decapentaplegic and wingless are regulated by eyes absent and eyegone and interact to direct the pattern of retinal differentiation in the eye disc. Development 125:3741–3751

4. Huppert SS, Jacobsen TL, Muskavitch MA (1997) Feedback regulation is central to Delta-Notch signalling required for Drosophila wing vein morphogenesis. Development 124:3283–3291

5. Sotillos S, de Celis JF (2006) Regulation of decapentaplegic expression during Drosophila wing veins pupal development. Mechanisms of Development 123:241–251

6. Ryoo HD, Domingos PM, Kang M-J, Steller H (2007) Unfolded protein response in a Drosophila model for retinal degeneration. The EMBO Journal 26:242–252

7. Wichmann A, Jaklevic B, Su TT (2006) Ionizing radiation induces caspase-dependent but Chk2- and p53-independent cell death in Drosophila melanogaster. Proceedings of the National Academy of Sciences 103:9952–9957

8. Tracey WD, Ning X, Klingler M, Kramer SG, Gergen JP (2000) Quantitative analysis of gene function in the Drosophila embryo. Genetics 154:273–284

9. Barrio L, Milán M (2017) Boundary Dpp promotes growth of medial and lateral regions of the Drosophila wing. eLife. doi: 10.7554/eLife.22013

10. Fritsch C, Sawala A, Harris R, Maartens A, Sutcliffe C, Ashe HL, Ray RP (2012) Different requirements for proteolytic processing of bone morphogenetic protein 5/6/7/8 ligands in Drosophila melanogaster. J Biol Chem 287:5942–5953

11. Tseng C-Y, Su Y-H, Yang S-M, Lin K-Y, Lai C-M, Rastegari E, Amartuvshin O, Cho Y, Cai Y, Hsu H-J (2018) Smad-Independent BMP Signaling in Somatic Cells Limits the Size of the Germline Stem Cell Pool. Stem Cell Reports 11:811–827

12. Isoo N, Sato C, Miyashita H, Shinohara M, Takasugi N, Morohashi Y, Tsuji S, Tomita T, Iwatsubo T (2007) Aβ42 Overproduction Associated with Structural Changes in the Catalytic Pore of γ-Secretase: COMMON EFFECTS OF PEN-2 N-TERMINAL ELONGATION AND FENOFIBRATE. Journal of Biological Chemistry 282:12388–12396

13. Haerry TE (2010) The interaction between two TGF-β type I receptors plays important roles in ligand binding, SMAD activation, and gradient formation. Mechanisms of Development 127:358–370

14. Haerry TE, Khalsa O, O'Connor MB, Wharton KA (1998) Synergistic signaling by two BMP ligands through the SAX and TKV receptors controls wing growth and patterning in Drosophila. Development 125:3977–3987

Supplementary Table 2. List of primers used for RT-qPCR.

Gene	Forward sequence (5' to 3')	Reverse sequence (5' to 3')
HLA-B27	GTGGGTCACGTGTGTCTTTG	ATTACATCGCCCTGAACGGA
HLA-B7	ACAAGGCTCAGGCACAGACT	GATGTAATCCTTGCCGTCGT
dad	TGATCGACGGAAGCGATCTG	CTGGACGTGCTGACTGGAAT
omb	TCTGGGCAGCGCCTATACTA	TTCTCCCACAGGTCTTTGCC
rho	GGTTCCACCTGGGCTTCAAT	GCCATGTAGATCACGCCGAT
kek1	GCAGTTCATCCGTGCGAATC	CGATTTCGCCGATCTTGCAG
sty	CGGTCATCGACTATGCCTCC	GGATTATCCACGCAGGGTGT
aos	TCGCCGGACTATAATGACGC	TGAATGTGGTTGCAGGCTCT
uba2	AGTCGTAGTAGATGCCGCACAG	TTCGGTTCATCCTCCTTGTCTT

Supplementary Table 3. Characteristics of SpA patients and healthy controls included in the p-Smad2/3 analysis by flow cytometry.

	SpA (N = 164)	Control (N = 16)
Age in years (mean ± SD)	49.6± 9.3	45.9± 14.9
Gender (Men/Women)	9/7	7/9
HLA-B27+ (%)	100	0
Disease duration in years (mean ± SD)	25.5± 10	N/A
SpA phenotype*		
AS (n)	10	0
Non-radiographic axial SpA (n)	6	0
BASDAI (mean ± SD)	2.9± 2.34	N/A
Treatment		
NSAID (n)	4	0
Anti-TNFα (n)	8	0
None (n)	5	14

All the SpA patients fulfilled the Assesment of SpondyloArthritis International Society classification criteria for axial SpA; [1] AS patients also fulfilled the modified New-York classification criteria; [2] non-radiographic axial SpA patients had no definite radiographic sacroliitis on antero-posterior pelvic radiograph.

BASDAI: Bath AS Disease Activity index; [3] NSAID: non-steroidal anti-inflammatory drug.
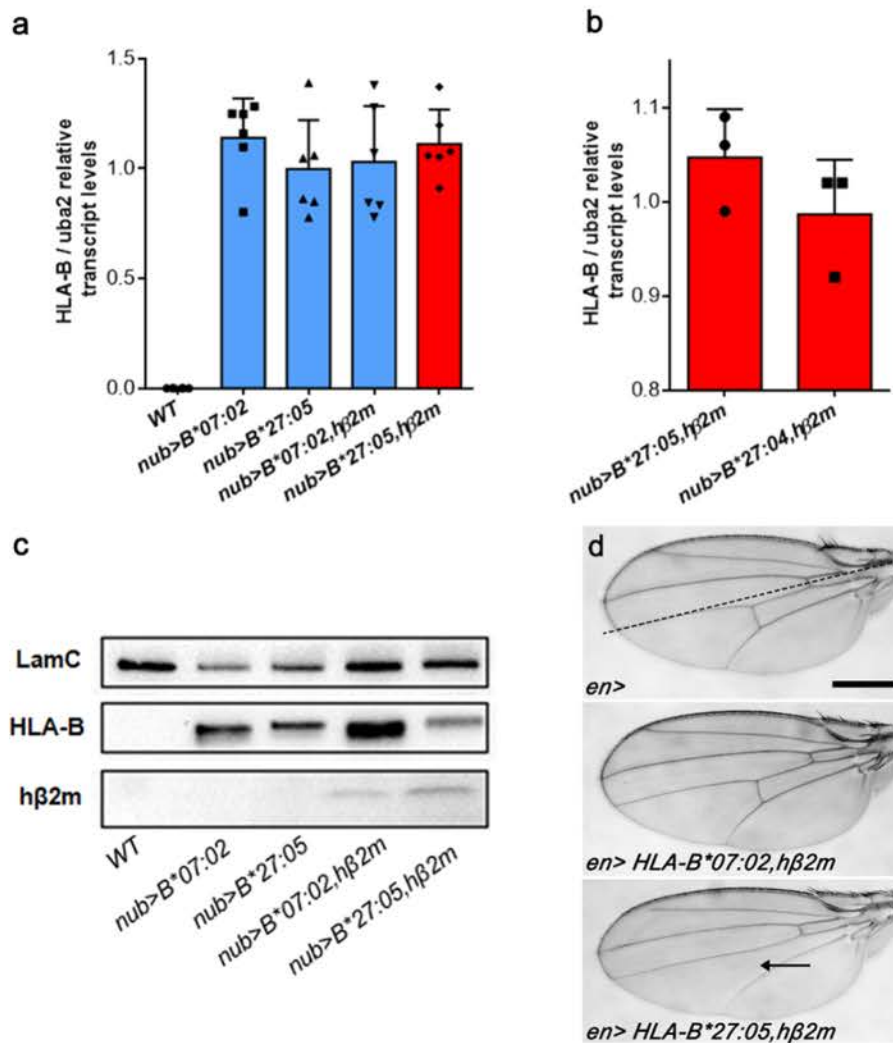
1. Rudwaleit M, van der Heijde D, Landewe R, et al. The development of Assessment of SpondyloArthritis international Society classification criteria for axial spondyloarthritis (part II): validation and final selection. Ann Rheum Dis 2009;68:777–83.
2. van der Linden S, Valkenburg HA, Cats A. Evaluation of diagnostic criteria for ankylosing spondylitis. A proposal for modification of the New York criteria. Arthritis Rheum 1984;27:361–8.
3. Garrett S, Jenkinson T, Kennedy LG, et al. A new approach to defining disease status in ankylosing spondylitis: the Bath Ankylosing Spondylitis Disease Activity Index. J Rheumatol 1994;21:2286–91.
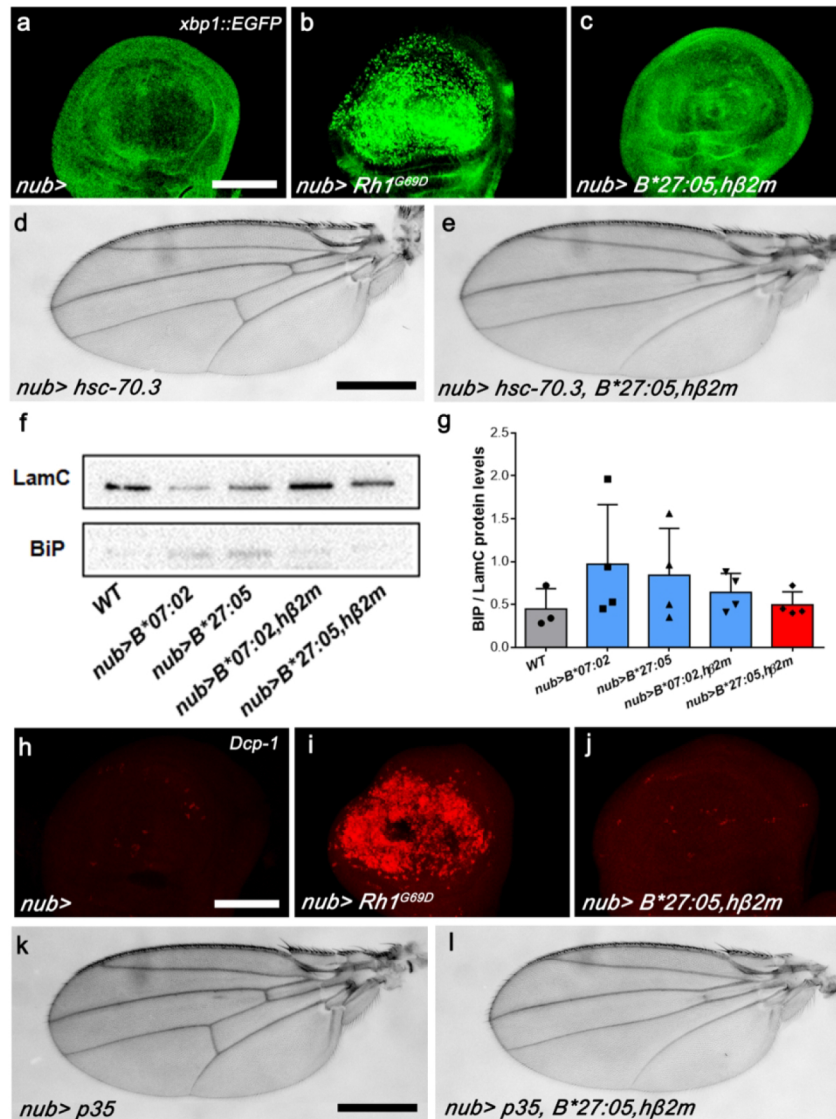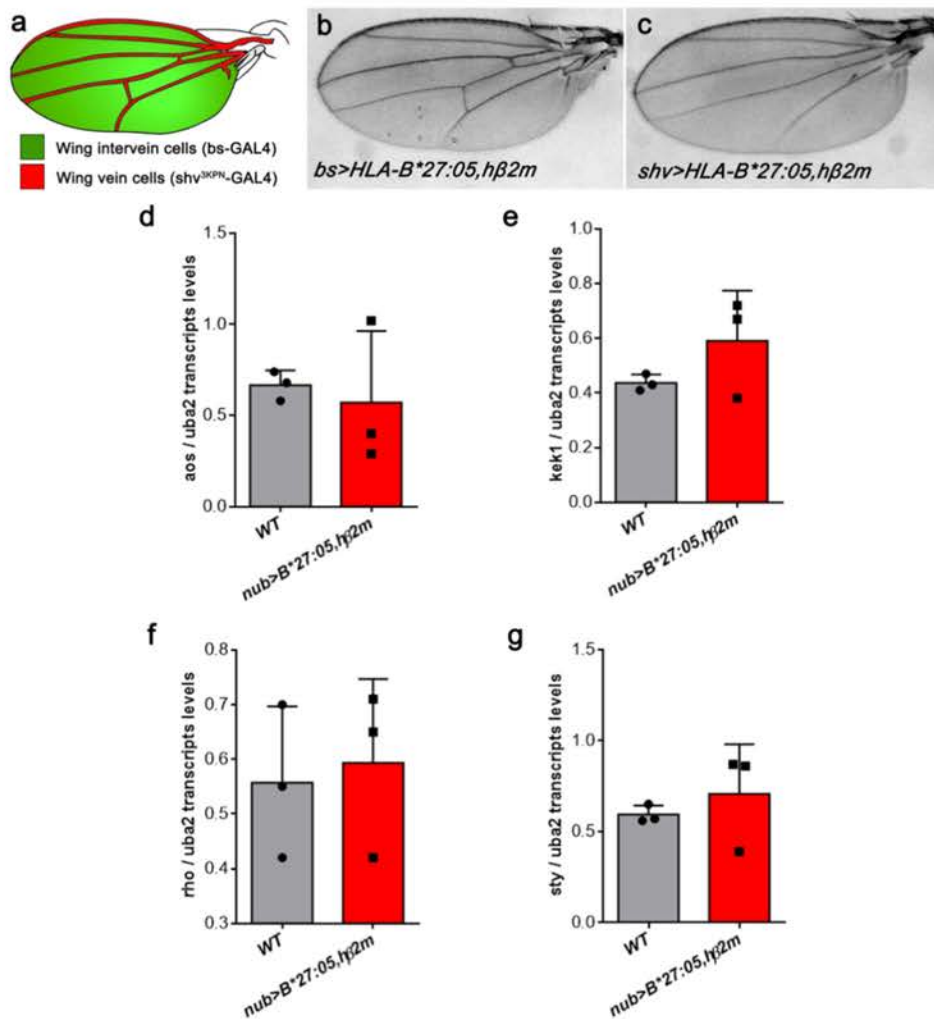
Supplementary Figure 1. Expression of HLA-B transgenes. (a, b) Levels of HLA-B transcripts driven by nub-GAL4 in the wing imaginal disc for different genotypes, relative to uba2 transcript levels. Graphs show the mean ± SEM of three independent experiments. Red bars indicate flies expressing both an AS-associated HLA-B27 allele and hβ2m. One-way ANOVA (excluding WT condition): p=0.61) **(a)**. Paired t-test: p=0.41) **(b)**. **(c)** Western-blot showing the HLA-B*07:02 and HLA-B*27:05 heavy chains at 44-45 kDa (HC-10 Ab) and the hβ2m light chain at 12 kDa (BBM1 Ab) in transgenic third instar imaginal wing discs. Lamin-C (LamC) was used as a loading control. **(d)** en-GAL4 was used to drive transgenes expression in the posterior compartment of *Drosophila* wing tissue. Scale bar: 200 μm. The antero-posterior frontier is indicated by a dotted line. Co-expression of HLA-B*07:02 and hβ2m was associated with normal wing aspect. Co-expression of HLA-B*27:05 and hβ2m resulted in posterior crossveinless phenotype (arrow).
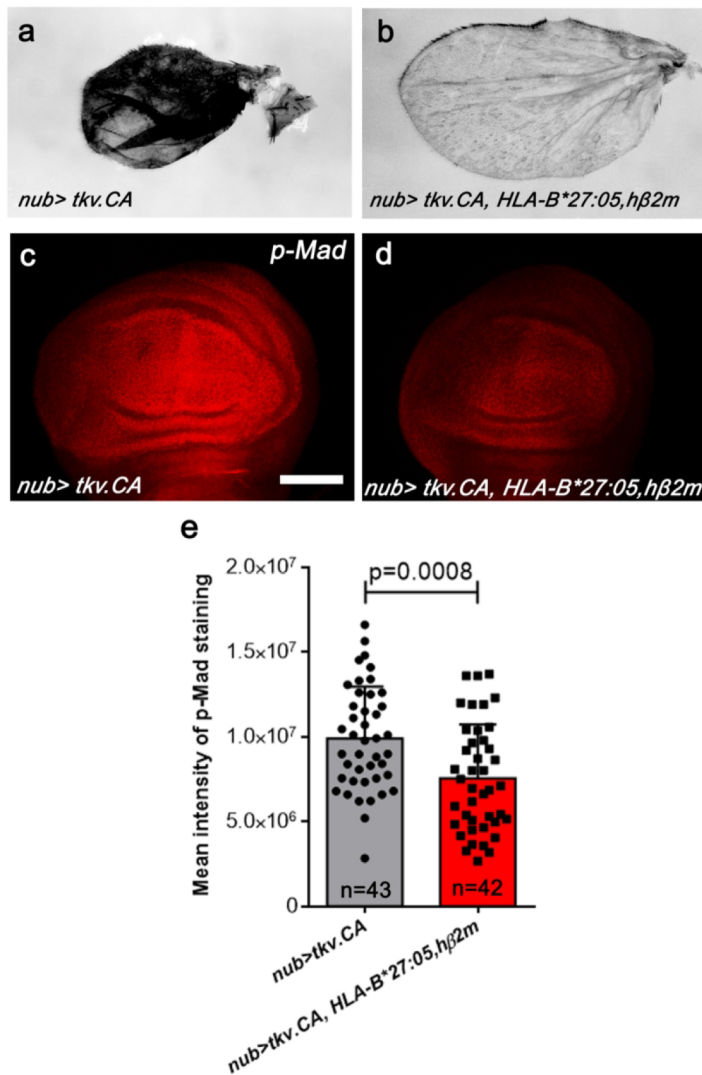
Supplementary Figure 2. The HLA-B27-induced crossveinless wing phenotype is neither associated with ER stress nor with cell death. (a-c) Projection from confocal stacks of third-instar larval wing imaginal discs carrying an xbp1::EGFP reporter transgene to detect ER-stress-induced UPR activation. Scale bar: 200 μm. No staining was observed with the negative control (nub-GAL4/+; xbp1::EGFP/+) **(a)**. Co-expression of a rhodopsin-1 mutant gene encoding an aggregation-prone protein was used as a positive control for UPR induction evidenced by dotted staining (nub-GAL4/+; xbp1::EGFP/UAS-Rh-1G69D) **(b)**. No staining was observed when HLA-B*27:05 was co-expressed with hβ2m (nub-GAL4/+; xbp1::EGFP/ UAS-HLA-B*27:05,UAS-hβ2m) **(c)**. **(d-e)** Overexpression of the ER chaperone Binding immunoglobulin protein (BiP, aka Hsc70-3 in Drosophila) does not suppress the HLA-B*27:05/hβ2m-induced crossveinless phenotype (nub-GAL4/UAS-BiP and nub-GAL4/UAS-BiP; UAS-HLA-B*27:05,UAS-hβ2m/+). **(f)** Detection of BiP in the wing imaginal disc by Western-blot as an ER stress marker. Lamin C (LamC) was used as a loading control. **(g)** Quantification of BiP relative to LamC levels in the wing imaginal discs. Each bar represents the mean ± SEM of three independent experiments. One-way ANOVA: p=0.45. The red bar indicates flies expressing both AS-associated HLA-B27 allele and hβ2m. **(h-j)** Cell death was detected in third-instar larval wing imaginal discs by immunostaining with anti-activated Death caspase-1 (Dcp-1; red). Scale bar: 200 μm. Genotypes are: nub-GAL4/+ (negative control) **(h)**; nub-GAL4/+; UAS-Rh-1G69D/+ (positive control) **(i)**; nub-GAL4/+; UAS-HLA-B*27:05,UAS-hβ2m/+ **(j)**. **(k-l)** The anti-apoptotic baculovirus p35 protein does not suppress the HLA-B*27:05/hβ2m-induced crossveinless phenotype in adult fly wings. Scale bar: 200 μm. Genotypes are: nub-GAL4/UAS-p35 **(k)** and nub-GAL4/ UAS-p35; UAS-HLA-B*27:05,UAS-hβ2m/+ **(l)**.

Supplementary Figure 3. HLA-B27:05/hβ2m-wing-phenotype is not associated with alteration of Notch or EGF signaling. (a) Schematic representation of the wing intervein and vein cells with the corresponding drivers, blistered (bs) and shortvein (shv) **(b)** bs-GAL4-driven HLA-B*27:05,hβ2m expression in wing intervein cells where Notch signaling is activated and required to prevent ectopic vein formation, does not lead to any wing phenotype. **(c)** shv3kpn-GAL4-driven HLA-B*27:05,hβ2m expression in wing vein cells resulted in the disappearance of both ACV and PCV. **(d-g)** Relative quantification of argos (aos), kekkon 1 (kek1), rhomboid (rho) and sprouty (sty) EGF-target genes transcripts from wing imaginal discs of nub-GAL4/+ (grey) or nub-GAL4/+; UAS-HLA-B*27:05,UAS-hβ2m/ + (red) genotype. Graphs show the mean ± SEM of three independent experiments. No significant difference was observed by unpaired t-test.

Supplementary Figure 4. HLA-B*27:05/hβ2m suppresses phenotypes induced by a constitutively active Tkv receptor. (a) Overexpression of a constitutively active form of Tkv results in a blistered and pigmented adult wing (nub/+; UAS-tkv.CA/+). **(b)** Genetic interaction with HLA-B*27:05/hβ2m attenuates the tkv.CA phenotype (nub/+; UAS-tkv.CA/UAS-HLA-B*27:05,UAS-hβ2m). **(c-d)** Immunostaining with anti-p-Mad in wing imaginal discs of the foregoing genotypes. Scale bar: 200 μm. **(e)** Quantification of p-Mad intensity in the previous genotypes. The graph represents the mean ± SEM. The p value of unpaired Student's t-test is shown.

Supplementary Figure 5. HLA-B*27:05 better folds and localizes to the plasma membrane than HLA-B*07:02. (a-c, e-g) Projections from confocal stacks of third-instar larval wing imaginal discs immunostained with ME1 **(a-c)** or w6/32 **(e-g)** anti-HLA-B mAbs recognizing well-folded HLA-Bs in wild-type (WT) condition (a, e), nub-GAL4/+; UAS-HLA-B*07:02,UAS-hβ2m/+ **(b, f),** and nub-GAL4/+; UAS-HLA-B*27:05,UAS-hβ2m/+ genotypes **(c, g)**. Fire LUT was used to indicate staining intensity. Scale bar: 200 μm **(d, h)** Mean fluorescence intensity of ME1 or w6/32 immunostaining. Error bars represent the SEM. The p values of unpaired Student's t-test are shown (ME1: Cohen's d=1.61 and w6/32: Cohen's d=0.82). **(i-j)** Percentages of wing imaginal disc cells with well-folded HLA-B, detected with ME1 **(i)** or w6/32 **(j)**, on their surface by FACS (n=3).

Supplementary Figure 6. HLA-B does not properly fold in the absence of hβ2m in *Drosophila* and hβ2m levels are not affected by the HLA-B type. Projections from confocal stacks of third-instar larval wing imaginal discs. Immunostaining with ME1 **(a-b)** or w6/32 **(c-d)** anti-HLA-B mAbs recognizing well-folded HLA-Bs in nub/+; UAS-B*07:02/+ **(a, c)** and nub/+; UAS-B*27:05/+ **(b, d)** genotypes. **(e-f)** Immunostaining with BBM1 anti-hβ2m Ab in nub/+; UAS-B*07:02, UAS-hβ2m/+ **(e)** and in nub/+; UAS-B*27:05, UAS-hβ2m/+ **(f)** genotypes. Fire LUT was used to indicate staining intensity. **(g)** Mean fluorescence intensity of BBM1 immunostaining. Error bars represent the SEM. There was no significant difference by unpaired Student's t-test.